A novel acoustic imaging tool for monitoring the state of rapid sand filters

Nihed Allouche, Dick G. Simons, Paul Keijzer, Luuk C. Rietveld and Joost Kappelhof

ABSTRACT

A new technology based on acoustic waves is developed to monitor the state of sand filters used in drinking water treatment. Changes in the sand filter, due to the removal of suspended particles from the water and their accumulation in the pores, result in an increase of the bulk density and acoustic speed of the granular material. Consequently, the reflected acoustic response changes as the filter is in use. To monitor these changes, an instrument composed of an omnidirectional transmitter and an array of hydrophones was built. With frequencies ranging between 10 and 110 kHz, high resolution is achieved in the vertical direction enabling the detectability of clogged layers with a minimum thickness of 1 cm. The novel instrument is tested by conducting a monitoring experiment in a filter used in practice. A 2D scan over a part of the filter was performed and repeated every 2 hours over a period of 10 days. An analysis of the data revealed a local increase of the reflected acoustic response with increasing filter run time. The changes in acoustic signal are mainly observed at the upper 5 cm of the sand bed. It is also clear that the filter bed is slowly compacting as a function of time. The total compaction after a period of 10 days reached 3.5 cm. The filter bed is expanded again during the cleaning procedure. Once the procedure is completed, the upper 30 cm of the filter becomes more transparent, showing small accumulations of material at greater depth. The observed changes in the filter bed demonstrate the potential of this acoustic-based tool to monitor the state of rapid sand filters and optimise their performance. The new tool can be used to evaluate the cleaning procedure and is valuable in detecting lateral variations in the filter bed. These variations may indicate local clogging that needs to be removed effectively to avoid deterioration of the overall performance in the long term. This type of information is difficult to obtain from the monitoring techniques currently used in drinking water treatment.

Key words | imaging, rapid sand filters, ultrasound

Nihed Allouche (corresponding author)
Dick G. Simons
Acoustic remote sensing group,
Delft University of Technology,
The Netherlands
E-mail: *nelallouche@hotmail.com*

Paul Keijzer
Electronic and mechanical support division,
Delft University of Technology,
The Netherlands

Luuk C. Rietveld
Department of Water Technology,
Delft University of Technology,
The Netherlands

Joost Kappelhof
Waternet,
The Netherlands

INTRODUCTION

Drinking water companies usually use sand filters for water treatment. Sand filtration is a rather simple process: the water is passed through a sand bed and suspended particles and microorganisms including bacteria are retained by the sand grains (Huisman 2004). These particles affect the properties of the filter and can cause its performance to deteriorate by blocking the water flow through the sand bed. Graded sand with an effective grain size of 0.35 to 2.6 mm is normally used for this purpose, sometimes with an additional coarser layer of material on top such as

anthracite. Deep-bed filtration occurs where particles accumulate over the entire depth of the filter bed. The filter grains are considered as collectors, whereas the accumulated particles will act as additional collectors, making the filtration step more efficient during the start-up phase (ripening period). The fluid velocity within the pores will increase as the particles accumulate and finally detachment will occur. Thus, in a filter layer that has reached a saturated but metastable configuration of deposits, attachment and detachment of particles will occur simultaneously

(Amirtharajah 1988). Finally filters are cleaned by reversing the flow direction, a procedure known as backwashing.

Employed often in drinking water production, rapid sand filtration is part of a wider water treatment process that needs to be monitored continuously. Typically, this is done by controlling the quality of the effluent by monitoring turbidity (Kim & Tobiason 2004). An increase in turbidity is associated with deterioration in the filter performance. Pressure measurements are conducted as well in order to monitor the state of the filter. Generally, this type of measurement serves as an indication of the amount of clogging in the filter bed. When a critical value is reached, the cleaning procedure is started. However, the pressure values are averaged over the whole filter bed and hence information on the local distribution of particle accumulations is not provided.

Some attempts were also made to record events in filtration and backwashing by applying video endoscopy (Ives 1989). However, these endoscopies have limitations in the optical resolution (Ives 2002). Samples from the sand bed are frequently taken to the laboratory for a more detailed analysis. This can take a few days whereas real time characterization is essential to reduce the risks and costs involved with water treatment. Long-term effects such as mixing of sand layers and the formation of mud balls are also not detected with the controlling and monitoring techniques used in practice. Therefore, Ives (2002) suggested using other techniques, such as tomography, to study filtration.

Acoustic imaging is a more suitable method to reveal the spatial distribution of clogging over the filter in time. Acoustic waves carry information about the media they travel through. They are reflected at boundaries representing a change in medium parameters. For a sand filter, this can either be a layer with a different grain size, grain material or a local accumulation of suspended particles in the pores. Despite their great potential, acoustic-based techniques are not yet fully explored as a monitoring tool nor widely applied for water treatment. Nevertheless, a few applications can be found in the literature. Acoustic waves were used by researchers to detect the distribution of immiscible liquids such as NAPL in a tank filled with sand (Geller *et al.* 2000). They showed that small NAPL saturations are easily detected from the amplitude of the acoustic waves. Another example involves a study of the effect of sediment-water interaction through ion exchange on acoustic wave propagation (Li & Pyrak-Nolte 2000). Here, a reduction in the acoustic wave amplitude was correlated with a decrease in the total number of ions in the pore water.

In this paper, we explore the potential of acoustic waves to monitor sand filtration by measuring the effect of clogging. An instrument, composed of an omnidirectional broadband transmitter and an array of hydrophones, was developed in order to test the method in practice. A monitoring experiment, using this novel instrument, was conducted on a full-scale sand filter during a complete filter run.

ACOUSTIC IMAGING OF SAND FILTERS

Acoustic imaging is a widely used technique based on the propagation of sound waves. These waves are mechanical disturbances that are carried through the inspected object and reflected at boundaries separating layers with contrast in density ρ and sound speed c. For a sand filter, these boundaries can either represent a sand layer with a different grain size and porosity or an accumulation of impurities that resulted locally in the clogging of the pores. The amplitude of the reflected signal depends on the contrast in acoustic impedance, i.e. the product of the sound speed and density, whereas its arrival time is affected only by the sound speed. Attenuation through homogeneous layers affects significantly the amplitude and the frequency content of the signal. Sound waves are attenuated by intrinsic absorption inherently present in the homogeneous medium and also by small-scale scattering (Lurton 2002). An increase of local accumulations in the sand layer is expected to result in stronger attenuation of the waves, thereby reducing their penetration depth.

In the water treatment process, suspended particles and colloidal solids are removed from the water and accumulated in the pores, which reduces the pore volume in the sand filter and hence the porosity. Consequently, the saturated bulk density of the sand, ρ_{sat} is expected to change with increasing run time of the filter. The saturated bulk density as a function of porosity can be computed using the equation

$$\rho_{\text{sat}} = n\rho_w + (1 - n)\rho_g \qquad (1)$$

where n is the fractional porosity, ρ_w is the density of the pore water and ρ_g is the bulk density of the mineral grains. The porosity affects also the sound speed as indicated by the Wood equation

$$c_{\text{sat}} = \sqrt{\frac{K_g K_w / ([n K_g + (1-n)K_w])}{\rho_{\text{sat}}}} \qquad (2)$$

where K_w and K_g denote the bulk moduli of the water and the sand grains in N/m^2, respectively (Stoll 2002). Both the saturated bulk density and the sound speed are expected to increase as porosity decreases (Hamilton 1980). This implies that the amplitude of the acoustic wave A_r, reflected at the top of the sand bed, also increases as shown by the following equation:

$$A_r = \frac{\rho_{\text{sat}} c_{\text{sat}} - \rho_w c_w}{\rho_{\text{sat}} c_{\text{sat}} + \rho_w c_w} \qquad (3)$$

where c_w denotes the sound speed of the water (Lurton 2002). In theory, this relation can be used to quantify the changes in density due to the filtration process from the measured acoustic response.

EXPERIMENTAL SET-UP

Instrument description

Based on the acoustic imaging principles described in the previous section, we developed an instrument that is able to image the state of a filter while in use. Figure 1 shows a schematic of the instrument, which is composed of an omnidirectional transmitter and a receiving hydrophone array. Both the signal emitted by the transmitter and the signal measured by each hydrophone are recorded. A dedicated software package has been developed to gain control of the parameters of the transmitted signal and visualize the recorded response. The transmitter sends out a chirp with linearly increasing frequency. This type of signal is chosen over a single frequency pulse in order to improve the vertical resolution of the images. In the case of a linear chirp, the vertical resolution

$$\Delta z = c/2B \qquad (4)$$

is inversely proportional to the bandwidth B, whereas the vertical resolution of a single frequency sinusoid depends linearly on the pulse duration. We typically sweep the frequency from 10 to 110 kHz. Assuming an average sound speed c of 1,500 m/s, this range of frequencies allows us to achieve a vertical resolution of approximately 1 cm. This implies that clogging in the filter bed of similar size can potentially be detected by the instrument.

The reflected signals are recorded by five hydrophones arranged along two perpendicular lines. The single hydrophones are omnidirectional. Using an array instead of a single hydrophone improves the sensitivity in the vertical direction and helps suppress undesired reflections arriving, in this case, from the sides of a filter. The response function of this array depends on the distance between the hydrophones, the frequency of the transmitted waves and the direction of the incoming wave.
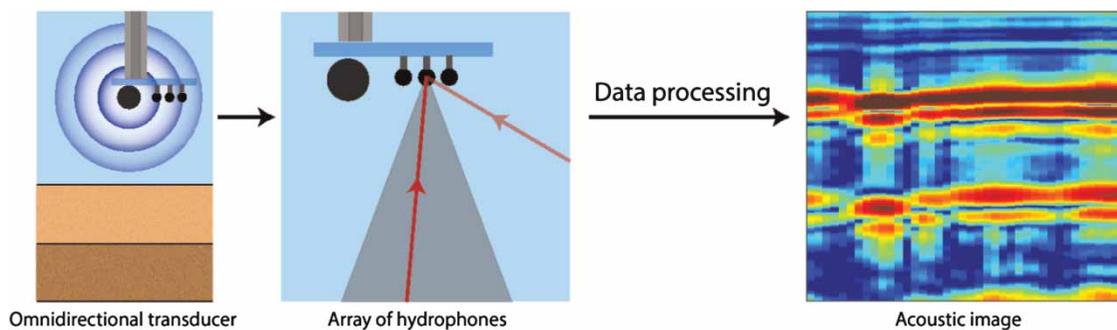

Figure 1 | A sketch of the developed instrument: an omnidirectional transducer sends a signal out which is then recorded by a hydrophone array with a beam opening angle of 34°. Reflections arriving outside the beam opening angle are strongly suppressed. The recorded acoustic signal is subsequently processed to a final image.

The distance between the hydrophones is 1.25 cm, corresponding to l/2 at a frequency of 60 kHz, with l being the wavelength. The −3 dB points of the response function defines the beam opening angle θ, which equals 34° at 60 kHz. The beam opening angle directly relates to the horizontal resolution of the instrument via

$$\Delta x = 2d \tan(\theta/2) \tag{5}$$

where d is the distance between the target and the hydrophone array. Extending the size of the array by adding more hydrophones will improve the horizontal resolution.

The transmitter and the hydrophone array are attached to a robot which can move in three directions along an aluminium frame. The robot is controlled via the computer and can be programmed to perform a scan in two directions and repeat it over a given period in time.

Monitoring experiment

To assess whether the developed instrument is able to detect changes in a filter used for water treatment, we performed a monitoring experiment in a rapid sand filter put at our disposal by a Dutch water company. The filter is used at the early stages of the water treatment process and is typically 156 hours in use before the cleaning procedure is started. The filter is about 10 m long and 5 m wide and is divided into two compartments separated by a channel built to drain water used in the backwashing procedure. The filter bed is 1.3 m thick and is composed of sand with a grain size between 0.8 and 1.25 mm. A stack of sand layers with increasing grain size is placed below the filter bed for support. Table 1 shows the composition of the filter bed material. The water height above the filter bed is 1.25 m

Table 1 │ Composition of the filter used in the experiment

Thickness [cm]	Grain size [mm]
130	0.8–1.25
15	1.25–2.0
15	2.0–3.0
15	3.0–5.0
15	5.0–8.0

and is variable during the filtration process. The instrument was placed on top of the filter as shown in Figure 2. The monitoring experiment was conducted over a period of 10 days where the state of the filter was imaged before the cleaning procedure and continued until a full cycle (period between two clean states of a filter) elapsed. A scan along the x-direction, indicated by the line in Figure 2, was repeated every 2 hours. The sensors were positioned 45 cm below the water surface and moved in 1 mm increments. A 90 cm long scan took about 15 min to complete.

Processing of the data

The signal emitted by the transducer is a 2 ms long chirp with a frequency range of 10 to 110 kHz. The chirp is compressed by applying a specific processing flow aimed at enhancing the vertical resolution of the recorded data. To this end, we use deconvolution to recover the impulse response and then apply a lowpass filter to reduce the artefacts introduced at the high frequencies. This is described by the following equation:

$$R(f) = F(f)\frac{D(f)}{S(f)} \tag{6}$$

where $S(f)$ is the spectrum of the chirp, $D(f)$ is the spectrum of the recorded signal, $F(f)$ is a low pass filter and $R(f)$ is the result. The processing steps are summarized in Figure 3: the chirp and the recorded signal are combined to obtain the final reflected response. The peaks obtained at the end of the processing flow are related to various arrivals reflected at boundaries with contrasts in acoustic properties. The described processing flow is applied to the sum of the five hydrophones and is repeated at recordings acquired at a horizontal increment of 1 mm. Figure 4 shows a typical image obtained for a 90 cm long profile (i.e. a stack of 901 transmissions). In this image, the depth axis is computed from the arrival time assuming a constant sound speed of 1,500 m/s. The reflection from the top of the sand bed is identified at a depth of 80 cm. Reflections from the water surface and the filter walls are also detected in the scan. They have a strong presence because of the large impedance contrast encountered at the water/air interface and the water/filter wall interface.
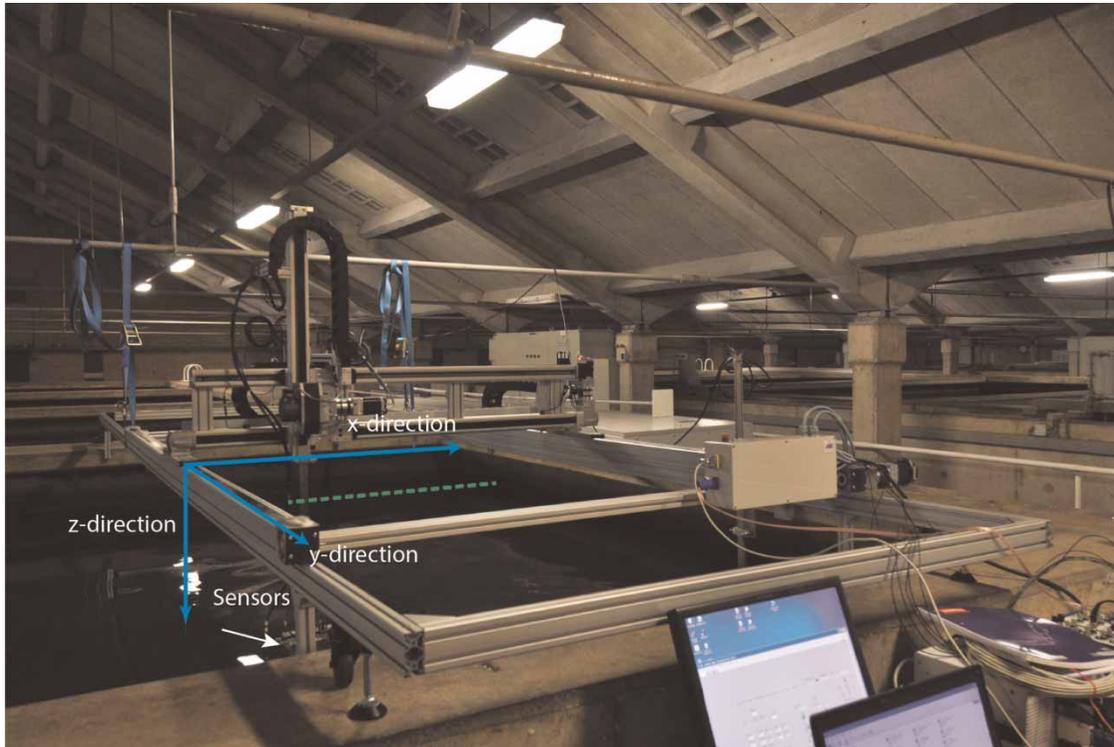
Figure 2 │ A picture showing the instrument placed on a sand filter. The line indicates the location of the scan.

However, they are not interfering with the reflection from the sand bed and can thus be removed from the scan. The monitoring experiment started by acquiring a scan of the filter which was already 4 days in use. After cleaning the filter by backwashing, the scans were repeated every 2 hours until it was cleaned again after 10 days.

RESULTS AND DISCUSSION

The results of the monitoring experiment are discussed in detail in this section. The changes in the measured acoustic signal, as a function of time and position in the filter bed, are presented. The observed acoustic changes are compared to pressure measurement and interpreted to obtain information on the filtration process and the state of the filter bed. The interpretation is supported by an acoustic modelling study which provides insights on the effect of clogging on the acoustic signal. The results are finally summarised in a sketch illustrating different stages of the filter bed during the experiment.

We start first by evaluating the effect of backwashing on the filter. This is done by comparing the images before and after the cleaning procedure. These images are displayed in Figure 5. It is clear that the amplitude of the signal, reflected at the top of the sand, decreased after backwashing. This was more the case in Figure 5(d) than in 5(b). This can be explained by the fact that the latter was scanned directly after the backwashing whereas the first scan was performed a few hours later. Another explanation could be that the cleaning procedure was shorter at the start of the experiment and therefore not all the impurities were removed.

Lateral variations in the amplitude of the reflected response were observed at the top of the sand bed. Some spots, indicated by the white circles, appeared to be more clogged than others. However, the locations of these spots were variable. They are impurities probably originating from deeper parts of the filter which were not entirely removed due to the limited duration of the cleaning procedure. When the flow direction was reversed, they ended up at a different location in the filter bed. From the data, we observed that these spots get clogged faster than other parts
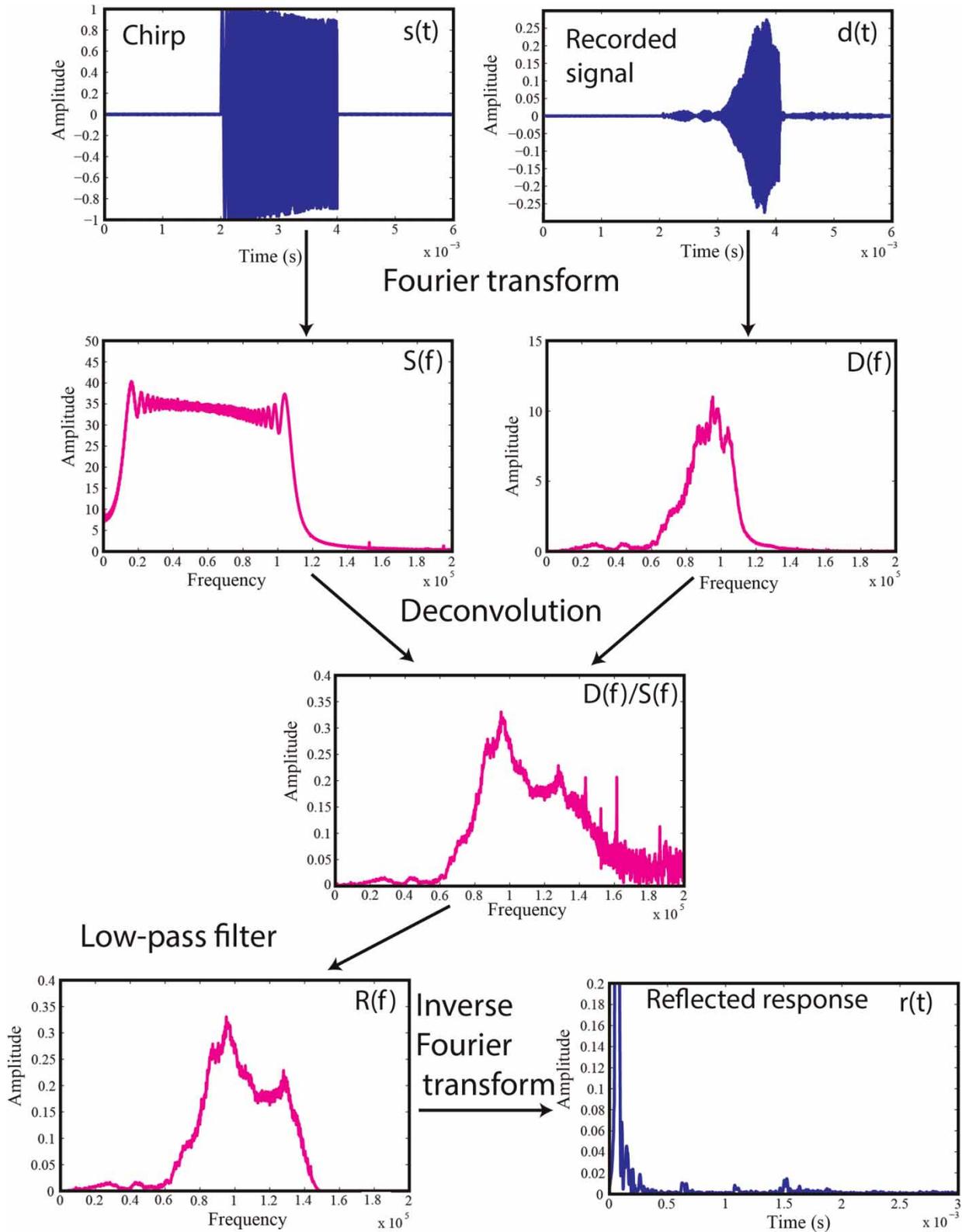
Figure 3 │ Processing flow applied to obtain a scan. The chirp (top left) and the recorded signal (top right) are transformed to the frequency domain where we apply deconvolution. The obtained spectrum is subsequently filtered and transformed back to the time domain.
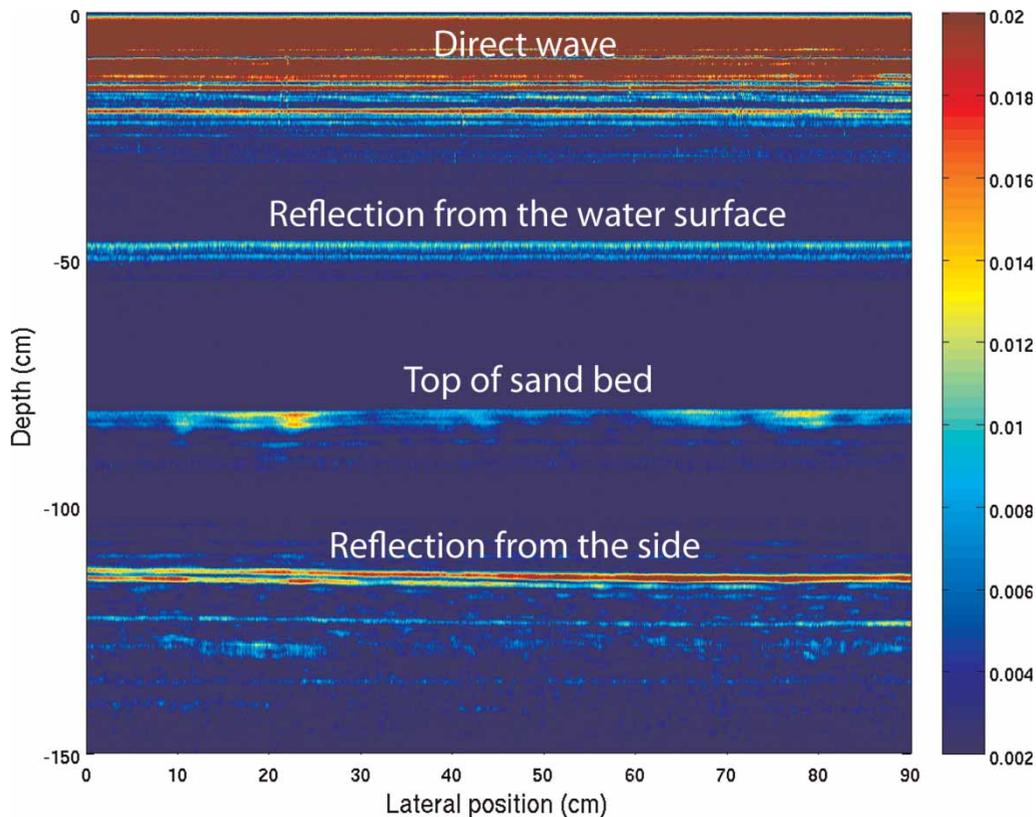
Figure 4 | An acoustic image of the filter obtained after processing and converting the arrival time to depth. The colour denotes the amplitude of the reflected signal. Four reflections are labelled: the direct wave, reflections from the water surface, top of the sand bed and the filter wall.

of the filter. This is because they acted as additional collectors, making it easier for suspended particles to be retained from the water (Amirtharajah 1988). As the filter was in use, the rest of the sand bed got clogged as well, increasing the amplitude of the reflected response as shown in Figure 5(c).

Small-scale variations in acoustic response corresponding to accumulations of impurities were distributed over the top 20 cm of the sand bed as it can be seen in Figure 5(b). These accumulations, with sizes in the order of a few centimetres, were only detectable shortly after backwashing. In the remaining scans of the filter they were masked by the strongly reflecting clogged top of the sand. The relative 'transparency' of the filter occurs only at the early stage of the filter run when the pores in the upper 5 cm of the filter were not clogged, allowing more acoustic energy to penetrate the deeper parts of the filter.

Scans of the filter were repeated every 2 hours. Figure 6 shows the changes in acoustic response with respect to time, averaged over the length of the profile for all scans. The direct wave and the wave reflected at the water surface are included in the figure to evaluate whether changes in the emitted signal or the water level have taken place. A clear trend, showing a slow compaction of the sand bed, can be observed, i.e. reflection from the top of the sand bed is placed at greater depths.

This effect is reversed when the cleaning procedure is started. The sand bed is then expanded.

A few hours after backwashing was completed, the depth of the filter bed stabilized. The variation in the depth of the sand bed as a function of time is plotted in Figure 7(a). Over a period of about 200 hours, the total compaction was 3.5 cm. The changes in the filter bed depth correlate well with changes in the pressure difference measured between two levels in the sand (Figure 7(b)). The water level, estimated from the acoustic wave reflected at the water surface, is plotted also in Figure 7(c). The water level is generally constant except for some jumps. The first jump, also visible in the pressure measurement, is associated
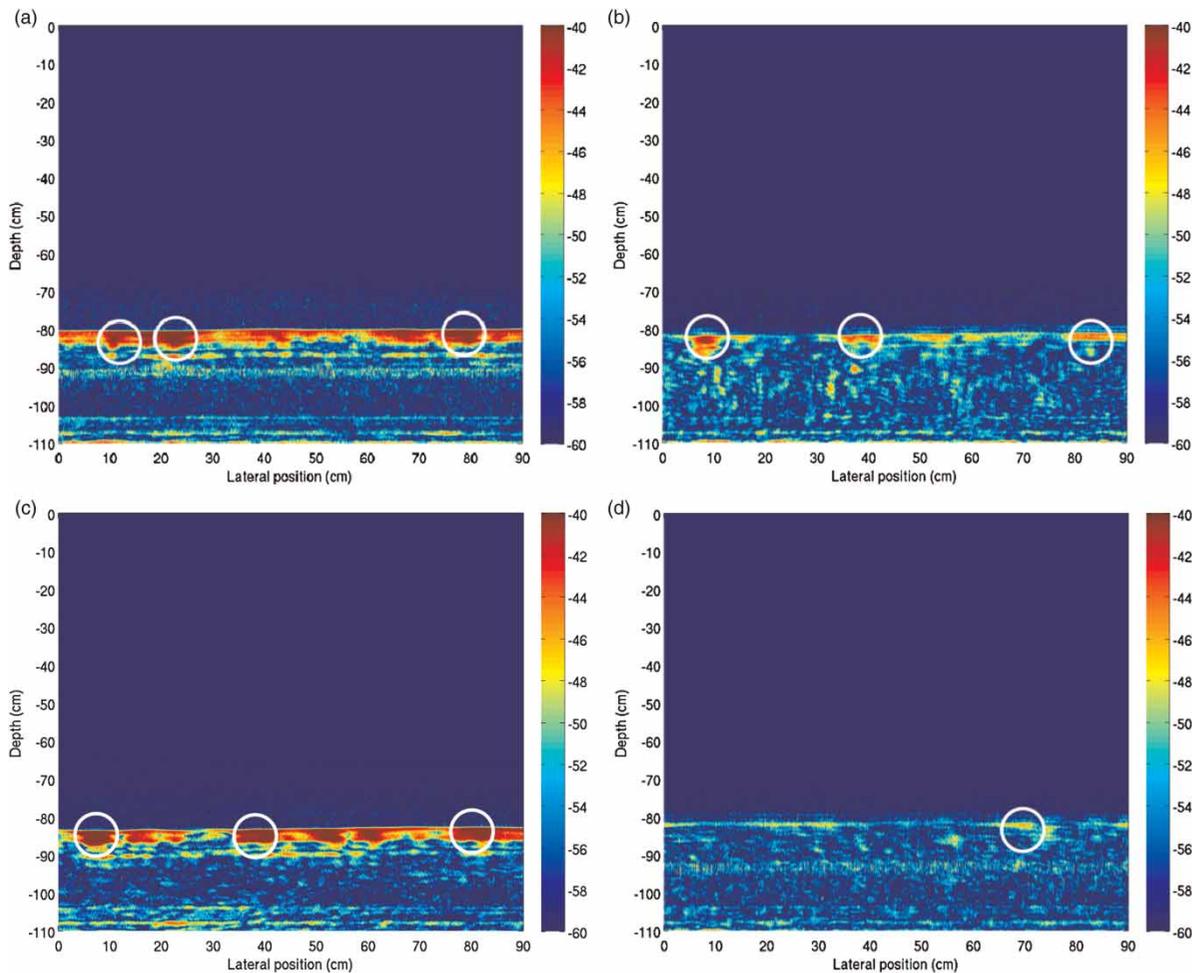
Figure 5 | Acoustic images of the filter: (a) at the start of the monitoring experiment, (b) after backwashing, (c) after 10 days of filter use and (d) after backwashing again.

with the backwashing of an adjacent filter. When one filter is not in use, more water is distributed over the remaining filters, thereby increasing the overall water level. There was a slight drop in the water level before it increased again at the end of the filter run time resulting in a large peak. This peak, which preceded the backwashing, can also be identified in the pressure measurement.

Due to lateral variations in the sand bed, the amplitude trend in Figure 6 is less obvious than that of the depth. Figure 8 shows an average image of the 90 cm long profile repeated for all days of the experiment. As the filter was in use, the clogged layer at the top of the sand bed became thicker as small-scale accumulations stuck together (compare Day 2 and Day 3). In the last 2 days of the filter run time, deeper clogging became more aligned forming another
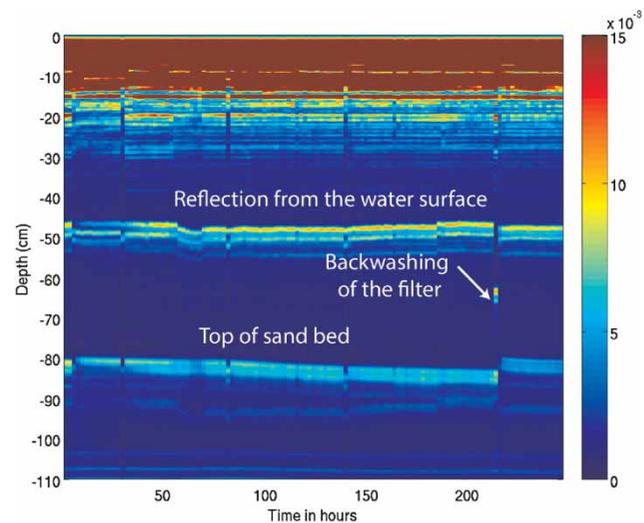

Figure 6 | The average acoustic response over the 90 cm long profile plotted for all scans performed every 2 hours.
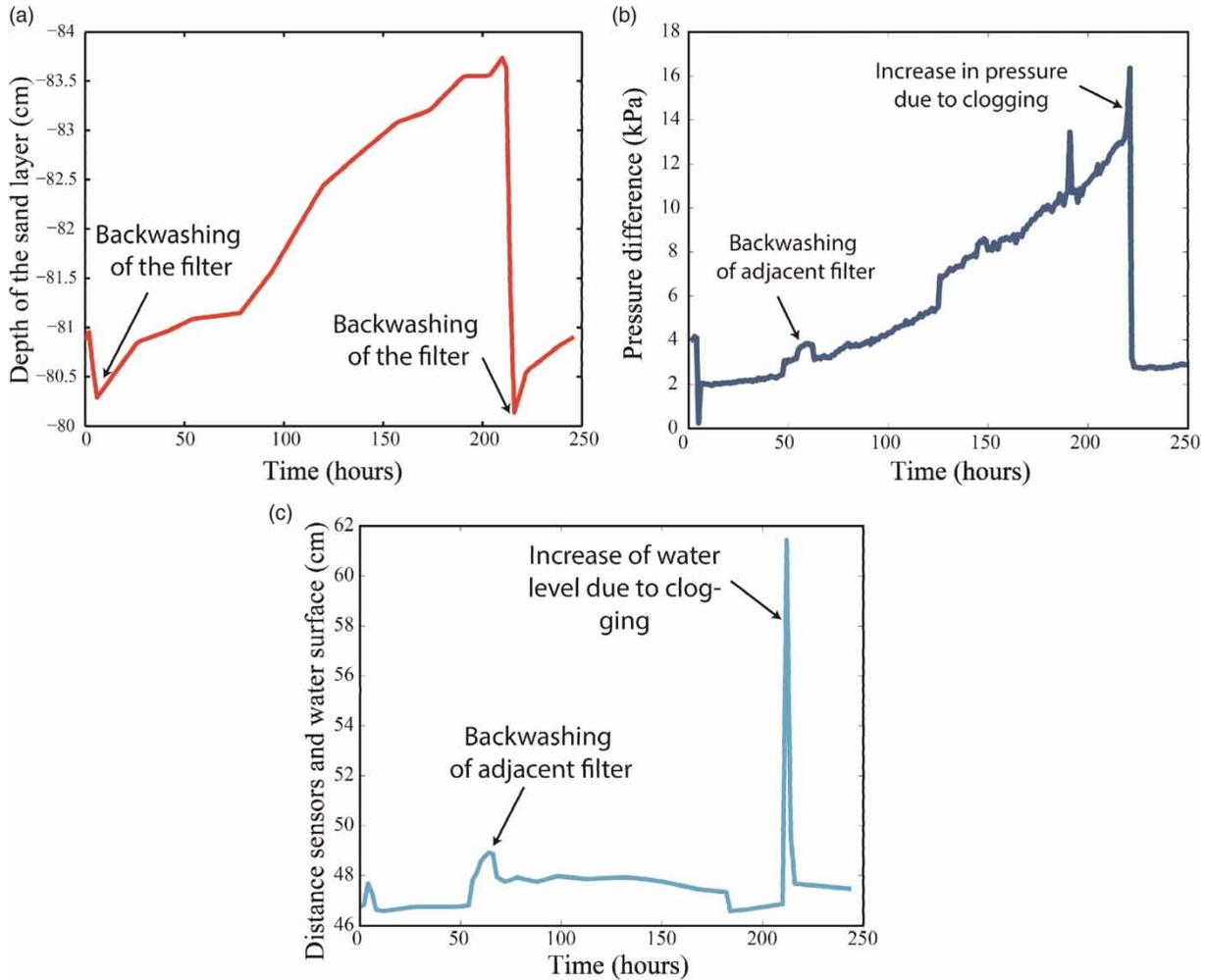
Figure 7 | (a) The average depth of the filter bed plotted for each scan. (b) The difference in pressure measured during the monitoring experiment. (c) The water level height above the sensors determined at each scan.
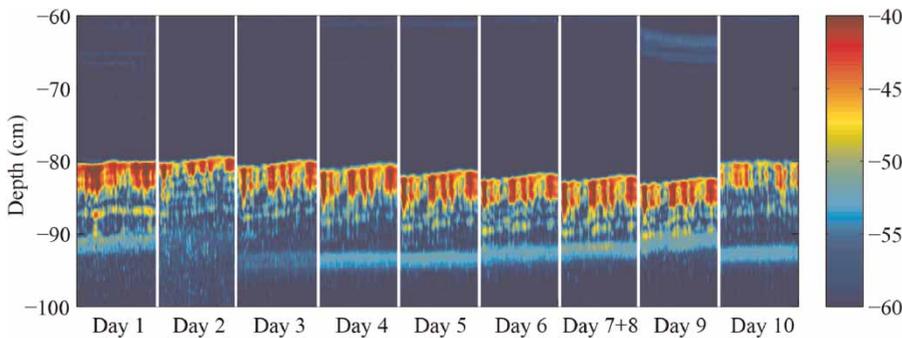

Figure 8 | Scans of the filter bed averaged from all measurements taken during 1 day.

clogged layer. As more pores were clogged in the upper part of the sand, the pore flow velocity increased and fewer solids accumulated there. Deeper parts took over until the filter resistance reaches a maximum. We observed that the clogging of the rapid sand filtration system mainly occurred in the top layer of the filter bed and the clogging zone gradually expanded when saturation occurred (equilibrium between attachment and detachment) (Amirtharajah 1998).

This is also indicated by the, more or less, linear increase of the pressure drop, since cake filtration on top of the filter bed will result in an exponential increase (Ives 2002) and strictly deep bed filtration in a quadratic increase.

Using acoustic modelling techniques, we can support the observations described above. The wavenumber integration method, also known as the reflectivity method, is selected for this purpose (Kennett 1983; Ursin 1983). Theoretically, the filter bed can be modelled as a stack of homogeneous layers with different acoustic properties. Attenuation is accounted for by making the sound speed complex valued. For simplicity, we model only the case of a plane wave incident vertically on the layered sand filter. A schematic of the sand bed used for the modelling is shown in Figure 9. Similar to the real filter, a 1.30 m thick sand layer with a grain size of 0.8 mm and a porosity of 0.37 is placed on top of a sand layer with coarser grains. The acoustic properties of the sand layers are taken from the literature (Jackson & Richardson 2007). The density of the sand grains is 2,670 kg/m^3 and the bulk moduli of the water and the grains are 2.2×10^9 and 4×10^{10} N/m^2, respectively. The source and receiver are located in the water at 80 cm distance from the top of the sand bed, as in the real experiment. The reflected response computed for the chirp with a frequency bandwidth of 10 to 110 kHz is also displayed in Figure 9. Three arrivals are visible: the direct wave, travelling directly between source and receiver, the reflection from the top of the sand bed and the reflection from the interface separating the fine and coarse-grained
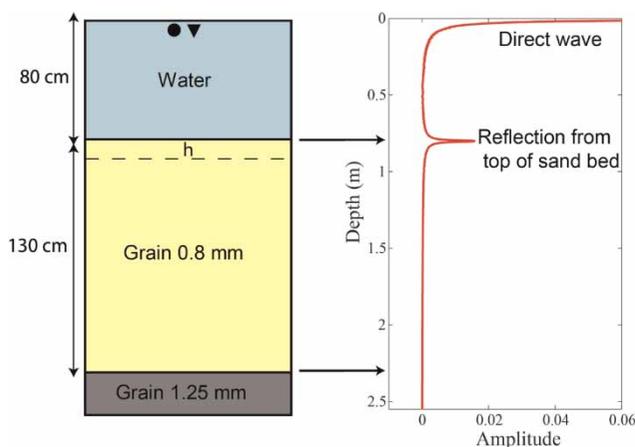
sands. The latter is not visible due to the intrinsic absorption in the sand layer. This explains as well why the reflection from the supporting layer in the full-scale sand filter was not visible in the data. Lower frequencies are required to detect it.

During filtration, most of the particles were retained first at the top of the sand bed as shown in Figure 8. This resulted in a thin layer with acoustic properties different from those of the clean sand bed. Corresponding changes in porosity affect the acoustic response. Figures 10(a) and 10(b) show the result of decreasing the fractional porosity from 0.37 to 0.3, 0.2, 0.1 and 0.05 for two layer thicknesses, 1 and 5 cm, respectively. When the clogged layer is as thin as 1 cm, the amplitude of the wave reflected at the top of the sand bed increased as the pore volume was reduced. This is consistent with the acoustic images shown in Figure 5 where the amplitude of the filter bed reflection increases with time as a result of clogging. The same effect occurs when the layer thickness is 5 cm. However, a second arrival with smaller amplitude also became visible. This corresponds to the reflection originating from the bottom of the clogged layer. The difference between the two figures is caused by the interference pattern. Obviously, the thicker the layer the better the top and the bottom are separated acoustically. In the experiment, this thickening of the clogged layer at the top of the sand bed occurred quite quickly (after a few hours). From Figure 10(b), it can also be noticed that the reflection from the bottom of the clogging was arriving earlier in time as the porosity decreased. The difference in travel time is caused by an increase in acoustic speed as predicted by the Wood equation (see Equation (2)).

Based on the above observations, provided by the acoustic measurement and supported by the modelling study, we can make a qualitative construction of the state of the filter during one run. First of all it must be noted that a small mass increase caused by the deposits, about 1–2% of the filter mass and resulting in a large hydraulic resistance (Mays & Hunt 2005), can be detected by the acoustic measurements. Further, Figure 11 illustrates different stages in the filter, starting after backwashing when small particles were left behind. As the filter is in use, more particles were accumulated in the sand but mainly at spots where the pore volume was reduced and the particles acted as additional collectors (Amirtharajah 1988). More particles were removed
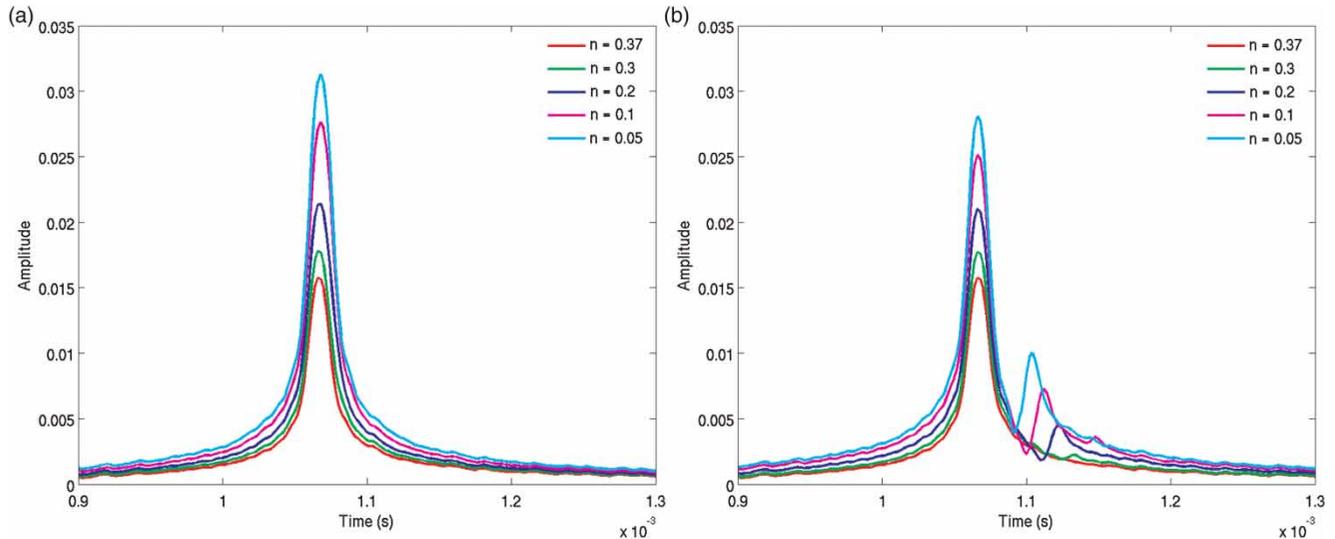
Figure 9 | The three-layered model used for the computation (left). The positions of the source and receiver are denoted by a circle and a triangle, respectively. The modelled acoustic response (right).

Figure 10 │ The effect of porosity on the acoustic response reflected at the top of the sand layer for a clogged layer with a thickness of 1 cm (a) and 5 cm (b).
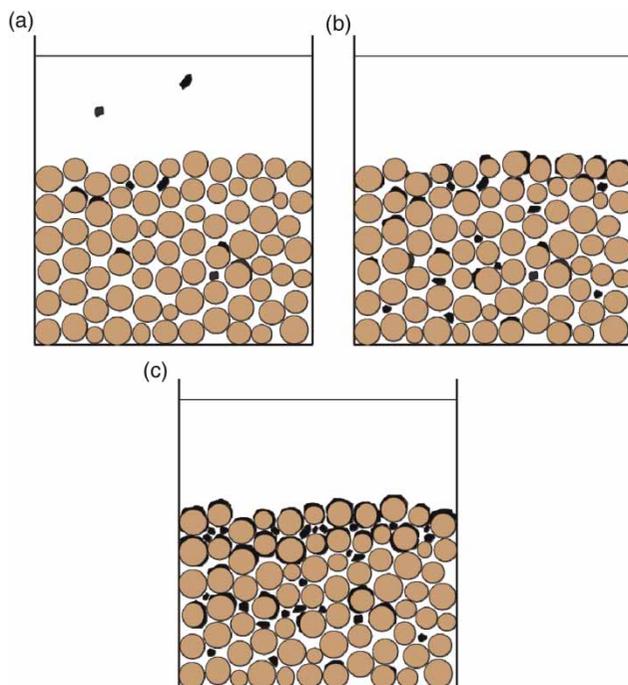

Figure 11 │ A schematic illustration of the different states of a rapid sand filter starting shortly after backwashing (a) and ending when the upper layer is clogged (c).

from water and accumulated in the upper part of the sand. Slowly this part became clogged and particles were deposited in deeper parts. The filter bed was slowly compacting. In the final stage, various clogged layers with decreasing thicknesses were formed. The information on the state of the

filter, described in detail in this section, demonstrates the great potential of the acoustic-based instrument as a monitoring tool. Images of the filter bed can be obtained anywhere in the filter bed. This can help in detecting local clogging that can cause the overall performance of the filter in the long term to deteriorate, e.g. through the formation of mud balls that are formed at the top and, in time, grow and sink to the bottom, clogging the water collection infrastructure (Brouckaert *et al.* 2006). The new tool can also be deployed to evaluate and optimise the cleaning procedure. In contrast to the pressure measurements, the information obtained is not averaged over the whole filter bed.

In the future, further improvements can be made to extract information from the deeper part of the filter and more effort can be put into the quantification of porosity changes and the detection of mud balls.

CONCLUSIONS

An acoustic-based instrument was developed as a monitoring tool for a water treatment process. This instrument, composed of a broadband transmitter and an array of hydrophones, was tested in an experiment conducted in a rapid sand filter used in practice. The state of the filter was monitored for a period of 10 days. As supported by the modelling study, an overall increase of the reflected acoustic

response was observed in the data. Acoustic waves are sensitive to changes in porosity. The density and acoustic speed increase when the water in the pores is replaced by suspended particles, thereby increasing the amplitude of the reflected acoustic response. The increase was mainly observed in the upper 5 cm of the sand bed. The performed scans showed also a slight compaction of the filter bed, when put in use, and expansion after backwashing was completed. Once cleaned, the upper 30 cm of the filter becomes 'transparent' and small accumulations of particles appear. These are not easily detectable because they are masked by the strongly reflecting clogged shallower part. It is clear that suspended materials are first retained at the top 5 cm of the sand bed before deeper parts take over. Furthermore, it can be stated that the backwashing procedure is very important because, if not performed properly (e.g. short duration), it may result in local variation in the filtering ability of the sand bed. This will affect the overall performance of the sand filter in the long term. The tool can then be used to optimise the cleaning procedure and detect variations in the quality of the sand bed. This information cannot be provided by the currently used monitoring techniques such as pressure and turbidity measurements.

ACKNOWLEDGEMENTS

REFERENCES

Amirtharajah, A. 1988 Some theoretical and conceptual views of filtration. *Journal of AWWA* **80** (12), 36–46.

Brouckaert, B. M., Amirtharajah, A., Brouckaert, C. J. & Amburgey, J. E. 2006 Predicting the efficiency of deposit removal during filter backwash. *Water SA* **23** (5), 633–640.

Hamilton, E. L. 1980 Geoacoustic modelling of the sea floor. *Journal of Acoustical Society of America* **68**, 1313–1340.

Huisman, L. 2004 Rapid filtration. Delft University of Technology Lecture Notes.

Geller, J. T., Kowalsky, M. B., Seifert, P. K. & Nihei, K. T. 2000 Acoustic detection of immiscible liquids in sand. *Geophysical Research Letters* **27**, 417–420.

Ives, K. J. 1989 Filtration studied with endoscopes. *Water Research* **23** (7), 861–866.

Ives, K. J. 2002 Filtration progress- more questions arising with fewer answers. *Water Science and Technology WS* **2** (1), 213–222.

Jackson, D. R. & Richardson, M. D. 2007 *High Frequency Seafloor Acoustics.* Springer-Verlag, New York.

Kennett, B. 1983 *Seismic Wave Propagation in Stratified Media.* Cambridge Univ. Press, UK.

Kim, J. & Tobiason, J. E. 2004 Particles in filter effluent: the roles of deposition and detachment. *Enviromental Science and Technology* **38**, 6132–6138.

Li, X. & Pyrak-Nolte, L. J. 2000 Acoustic monitoring of sediment-pore fluid interaction. *Geophysical Research Letters* **25**, 3899–3902.

Lurton, X. 2002 *An Introduction to Underwater Acoustics: Principles and Applications.* Springer-Praxis, UK.

Mays, D. C. & Hunt, J. R. 2005 Hydrodynamic aspects of particle clogging in porous media. *Environmental Science and Technology* **39**, 577–584.

Stoll, R. D. 2002 Velocity dispersion in water-saturated granular sediment. *Journal of Acoustical Society of America* **111**, 785–792.

Ursin, B. 1983 Review of elastic and electromagnetic wave propagation in layered media. *Geophysics* **48**, 1063–1081.